The function of estuaries mixing zones in main productivity and nutrient flow of coastal waters

Debarghya Biswas[1]; Ankita Tiwari[2]; Dr. Sushma Murlie[3]

Received: 01 March 2025; Revised: 03 April 2025; Accepted: 19 April 2025; Published: 20 May 2025

Abstract

Estuaries are centers of primary production and nutrient conversion that enhance food webs and environmental functionality locally and in the surrounding environments. The depth-dependent nutrient conversion and main productivity processes in the water column and seafloor were examined, and the lateral flow of substances and materials through the estuary mouth was determined. As a case study, the impacts of Sea Level Rise (SLR) on production and nutrient changes were anticipated using an estuary characterized by shallower soft-sediment ecosystems. The estuary functioned as a net recipient of dissolved minerals from the coast while simultaneously acting as an indirect export of suspended material and chlorophyll a, reinforcing that estuaries serve as significant nutrient transformation processors. A substantial depth (and light) influence on productivity suggests that escalating environmental obstacles, which diminish light at the seafloor (SLR and heightened turbidity), adversely affect estuarine production. Tidal and weak subtidal benthic ecosystems accounted for most of the estuary's efficiency, a trend likely applicable to other weak estuaries worldwide. SLR and human interventions that inhibit landward emigration, such as seawalls and armoring, will lead to the degradation of these environments and their essential benefits to neighboring coastal environments.

Keywords: Estuaries, Productivity, Nutrient flow, Coastal waters

1- Assistant Professor, Department of CS & IT, Kalinga University, Raipur, India.
Email: ku.debarghyabiswas@kalingauniversity.ac.in, ORCID: https://orcid.org/0009-0004-0730-9948
2- Research Scholar, Department of CS & IT, Kalinga University, Raipur, India.
Email: ankita.tiwari@kalingauniversity.ac.in, ORCID: https://orcid.org/0009-0007-5517-3848
3- Associate Professor, New Delhi Institute of Management, New Delhi, India.
Email: sushma.muralie@ndimdelhi.org, ORCID: https://orcid.org/0000-0002-3878-8046
DOI: 10.70102/IJARES/V5I1/5-1-50

Introduction

Estuaries are recognized as some of Earth's most dynamic and productive ecosystems (Cardoso, 2022). Estuaries frequently harbor substantial quantities of fresh and decomposing organic carbon, with an opportunity for a net export of these substances to neighboring coastal ecosystems (Rahman *et al.,* 2024). Mangroves, marsh grasses, and seagrass prairies are prominent sources of temperate coastlines' main organic carbon generation. These plant varieties offer critical habitats for numerous esteemed bird and aquatic species. In multiple regions globally, the predominant source of primary productivity in estuarine benthic organism ecosystems is microphytobenthos (biofilms consisting of photosynthetic bacteria and microbes), rather than extensive emergent plants, owing to the superior areal coverage and depth spread of microphytobenthos compared to macrophytes.

The significance of intertidal and deep subtidal ecosystems for producing primary products and enhancing resistance to estuarine shocks is widely acknowledged (Mustafa *et al.,* 2024). The regrowth of inorganic nitrogen (N) and phosphorus (P) in dirt grants benthic leading producers a source of essential nutrients, and deep waters offer greater light availability at the seabed compared to deeper waters due to the diminution of light as it penetrates the water column. In estuaries characterized by tidal and deep subtidal soft-sediment condominiums, benthic primary output can significantly surpass the efficiency of phytoplankton in the water column (Smihunova *et al.,* 2024). Microphytobenthic production is believed to sustain robust macrofaunal neighborhoods, especially livestock and feeders of deposits that consume new continental organic matter (Mthembu and Dlamini, 2024). The capacity for the conveyance of this output (i.e., export from the estuary outlet) is significantly less than that of phytoplankton-derived production (Costa *et al.,* 2023).

The equilibrium between the water columns and benthic manufacturing and the extent of estuarine subsidies to the neighboring coastal zone will differ from one estuary to another (Rullens *et al.,* 2022). This is due to the distinct ratios of hollow to deep water, varying levels of dispersed and particulate substances that diminish light, differing tidal exchange scales that influence the mixing of stream and ocean components, and variations in contact with wind- and storm-induced waves that can impact particle settling rates (Farfoura *et al.,* 2023). These traits will influence the reactions of estuaries to widespread stresses such as terrigenous silt influx from coastal streams and Sea Level Rise (SLR) (Patankar and Kapoor, 2024). Climate warming is anticipated to elevate the worldwide average sea level by 0.4 to over 1.2 meters by 2120. Since depth and corresponding light penetration are critical factors affecting photosynthesis and other essential activities, SLR could substantially alter estuarine function and ecology. A crucial element influencing the effect of SLR on estuarine output is the estuary's capacity to extend outward (Shakya and Allgeier, 2023). Landward growth is dictated by the water level or geography (hypsometry) and the extent of armoring (e.g., by seawalls) of the estuary's land-sea boundaries. Variation in hypsometry and manmade factors, such as the armoring of estuarine shorelines, will likely lead to substantial disparities in estuarine reactions to SLR, affecting their utilization and management (Gonzalez and El-Sayed, 2024). The research performed a case study to evaluate the comparative significance of benthic vs aquatic initial production in a deep, unvegetated harbor in northern the country. The research analyzed tidally driven laterally material fluxes near the estuary's entrance (Ranjan and Bhagat, 2024).

The research integrated this with SLR forecasts to evaluate potential alterations in estuarine production resulting from changes in the area of deep bottom habitats. The predominant feature of Mahurangi Harbor consists of shallow soft-sediment ecosystems (tidal or <5 m below Lower Astronomical Tides) devoid of macrophytes (Robles *et al.*, 2015; Myoa, Pyo and Mon, 2023). The water level at the estuary's reference, characterized by a moderately deep core channel next to shallow edge habitats, was conducive to a concurrent examination of the depth-dependent relationships between benthic and aquatic primary production and chlorophyll existing stocks (Dias *et al.*, 2023; Akyol and Capape, 2024).

The primary aim of the research was to enhance comprehension of estuary productivity's response to evolving stresses, including heightened turbidity and SLR, thereby informing potential management strategies (Nihlani and Chhabda, 2024; Agarwal and Yadhav, 2023). To achieve this goal, the study encompassed numerous interconnected aims. The first objective was to contrast the current stock of new microalgal biomass in the water stream and on the seafloor (Soares, Galiforni-Silva and Winter, 2024). The following objective was to contrast the photosynthesis rates, oxygen generation, and the corresponding uptake of soluble organic nutrients by microphytes in the water columns and the bottom (Iyengar and Joshi, 2024). The third purpose was to conduct the aforementioned observations at various depths to ascertain the influence of depth on the relative equilibrium between the water's level and benthic production. The primary objective of the investigation was to quantify the net outflow of soluble and particle suspension pollutants from the harbour (Robles *et al.*, 2015). This necessitated comprehensive evaluations of the substances within the water's pillar at various depths and tidal conditions, along with data on the amount of water entering or exiting an estuary at particular depths and periods. By contextualizing the research's findings with SLR forecasts, the study emphasizes the significance of SLR for primary manufacturing at the intertidal scale in this river (Khojasteh *et al.*, 2021; Arvinth, 2023).

Incorporation and Parameterization of Models

This study's integrative modeling method included climate situations, a GIS climate device, and watersheds and environmental models, as illustrated in Figure 1. This section provides a detailed description of the incorporation of tools and designs, as well as the setting of parameters of systems.

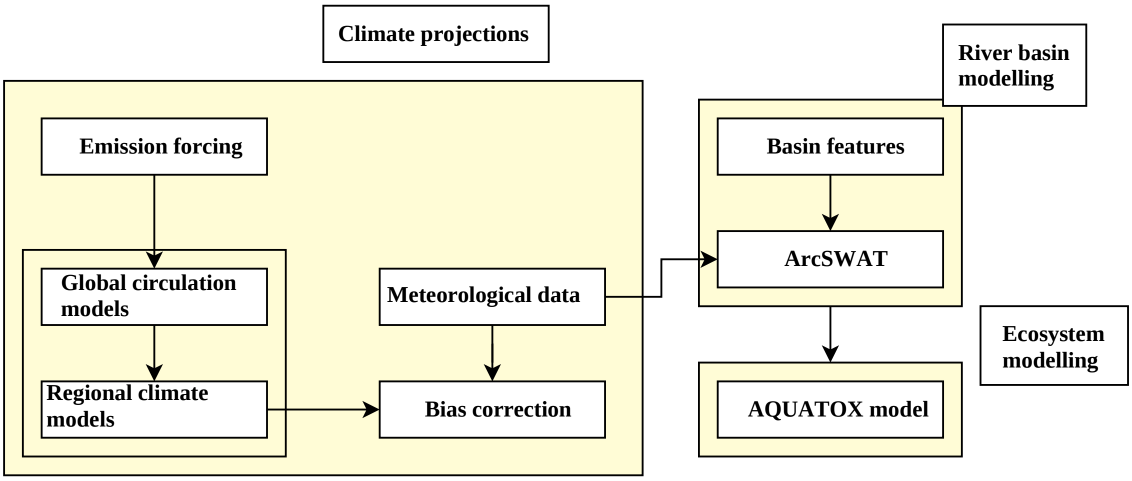

Figure 1: Structure of the study.

Climate Projections

This investigation exclusively examined alterations in temperatures and rainfall. The anticipated modifications in temperatures and precipitation were derived from the climatic scenarios produced under the RCP4.6 and RCP8.7 emission predictions. The chosen situations possess a horizontal accuracy of 0.08° (6 km) and were employed to contrast the 30-year reference period from 1980 to 2018 with the climate forecasts for the mid-term from 2042 to 2080 and the long-term from 2070 to 2120. The Global Information System (GIS) tool CLImate Modelling Environment (CLIME) juxtaposed the spatial grids of values found (i.e., weather sensors) with the geographical grid of the situation at hand for the controlling time and implemented the linear-scaling bias-correction procedure. The derived delta variables for every month were then transferred to future periods, yielding bias-corrected daily readings for temperatures and rainfall utilized as input for the Soil and Water Assessment Tool (SWAT) and AQUATOX.

Simulation of the Zambezi River Basin

The hydrological and water quality parameters of the Zero River were simulated using SWAT with the subsequent data: Daily intervals of meteorological information (i.e., precipitation, temperatures, wind, sunlight, and relative moisture) from three weather observatories for the years 2005-2020; a 6x6m digital rising approach; a 120x120m land-use relate; a 550x550m soil define detailing geomorphological and textural features; agricultural administration actions for chosen crops (corn, soybeans, winter grain); a daily parallel of stream flow from one measuring location for the duration 2005-2020; daily time parallel of organic nitrogen levels (i.e., nitrates and ammonium) for the period 2006-2020. The absence of ongoing, high-frequency series information on phosphorus levels precluded verification and calibration of phosphate loading. Despite being perceived as a possible cause of unpredictability, the juxtaposition of predicted values with average annual information from 2000, derived from a prior study, facilitated a qualitative analysis of the yearly average and seasonal variations.

Owing to the absence of continuous information, the impact of recharging groundwater from the adjacent basins was simulated with an added constant component. The effect of point-source contamination (wastewater treatment plants, industrial outflows) on nutrient loads was modeled with a continuous input. Values were derived from prior investigations.

The SWAT strategy was executed from 2005 to 2020, incorporating a three-year warming-up time. The calibration phase was established from 2005 to 2010, while the testing period was from 2010 to 2020. The SWAT framework generated regular results for the release of water (Q), the nitrogen from nitrate (N-NO3), ammonia (N-NHa), and phosphorus from orthophosphate (P-POA), which were utilized as inputs for the AQUATOX system.

Ecosystem Modelling

An AQUATOX modeling software was utilized to depict phytoplankton behavior and structure in PdC. The region has been modeled as a confined aquatic system exclusively affected by the groundwater outflow from the Zero River basins. The influence of tides has been disregarded to prevent additional complications. This ought to be regarded as a possible cause of confusion. The subsequent parameterization information was utilized: The modelled area measures approximately 5 km in length (L), 1.4 km in width (W), with a mean depth of 0.9 m (H) and a highest depth of 3.4 m (Hmax). The volume (V) of the network was maintained at a constant 4.2×10^6 m³; monthly averages of water outflow (m³/s) and nutrient loading (kg/month) were derived from the SWAT model of the Zero River watershed. Every month, temperatures of the water principles were sourced from the tracking system from 2008 to 2015. The mean yearly and variation in wind speed (m/s) and the amount of light at the surface (Lux/day) were calculated using weather information from the same period. A steady pH value of 7.8 was assumed. Chemical variables, including chemical nitrate and phosphorus levels (mg/L), Dissolved Oxygen (DO), and saltiness, were gathered from the tracking effort and system. Total Stopped Solids (TSS) were established at 9 mg/L. This number is derived from mean measurements under tranquil conditions (ignoring the influence of wind and waves) in the lagoon.

The simulated ecosystem consists of trash, phytoplankton, and crustaceans. Detritus is categorized into suspended particles, intermittent detritus, suspension particle labile trash, intermittent sediment, unstable sediment, and soluble debris. Due to the absence of site-specific data, no modeling was conducted. Nine phytoplankton sections, comprising seven Diatoms (D) and one Cyanobacteria (CB), were incorporated to illustrate the potential developments of the algae biomass and structure under current and future circumstances. The investigation identified the default creatures in the AQUATOX library that exhibit the most comparable features to the organisms found in the waterways of Venice. Navigation and Cyclotella taxa are prevalent in the seawater of the lagoon. Fragilaria sp. was identified as a species present in intermediate water environments. A type of Cyanobacteria was utilized to determine whether future ecological situations might promote cyanobacterial blooms. The genus Microcystis sp. was chosen from the AQUATOX collection for its notable salt tolerance and capacity to manufacture microcystin poisons that exhibit stability and persistence in transitional environments.

Modeling Presumptions and Qualifications in Prospective Situations

Certain assumptions and cautions were considered to replicate the physicochemical and ecological parameters of the study area. The remaining climatic factors, namely, speed of the wind, sun radiation, and humidity ratio, were maintained at the same levels. The statistical characteristics of the information collected during the calibration and verification periods were utilized in the SWAT Forecast Maker to provide daily information by rainfall and temperature. In AQUATOX, the calculated mean and variation in wind velocity and ultraviolet radiation were maintained constant throughout mid- and long-term durations. Secondly, land use, farming methods, and other greenhouse gases in the Zero Rivers basin have remained steady, including wastewater treatment plants and factory discharges. Third, the impacts of rising seas and human facilities, such as the MOSE construction at the lagoon inlets of Italy, have been overlooked. In conclusion, due to the lack of high-resolution water temperature forecasts for the canal of Venezia under RCP4.6 and RCP8.7, the predicted water temperatures were derived by a regression analysis correlating monitored air temperatures with water temperatures.

Results

Laboratory Amalgamation Test

The study of the mixing theory for the occlusion test revealed that three component end-members accounted for 84.2% of the overall variance in the particle size distributions. The end-member sizes exhibited modes at 9 µm, 135 µm, and 195 µm, contributing 38%, 31%, and 27% to the explanatory variation. The volume percentages of the size of particle categories associated with the modes of recognized end-members exhibited unique behavior during the mixing operation. The fraction of the smallest molecules in the overall particle quantity diminished during the investigation, while the fraction of the larger particles increased. Particles of various sizes attained a maximum percentage at a salinity of approximately 2 g kg-1, after which the ratio diminished. During the study, the total volumetric concentration that contained particulates rose exponentially from less than 10 to greater than 42 µL-1. The average size rose at the onset of the salinity gradients but stabilized after reaching a salinity of 2.7 g kg-1. Humic-like luminescence, turbidity, and pH were elevated throughout the experiment.

Particle phosphorus and iron in the narrowest size class (1-5 µm) exhibited a notable increase with rising salinity. The linear rise in the lowest particle P size fraction ranged from 0.04 to 0.06 umol/L, while for Fe, it increased from 1.7 to 2.4 umol/L. Other factors and size categories did not produce notable patterns.

Empirical Observations

During the sampling period, salinity stratification was detected across the estuary. The first 10 meters of the water column had a 3-5 g kg^{1} salinity, but the deeper levels (subhalocline) exhibited a 4-6 g kg^{1} salinity. A narrow lens with saline 1-5 g kg^-1 stretched from the entrance of the Karjaanjoki River to an extent of 6 km downriver. In contrast, waters with salinity exceeding 7 g kg^-1 were observed on the outside margin of the sill. Oxygen levels were significantly diminished in the subhalocline liquid mass, attaining values below 1 mg/L at depths exceeding 25 m. A comparable disparity among top and subhalocline was noted in luminous DOM, chl-a, and pH, all exhibiting elevated values in the water column. These metrics exhibited unique lateral patterns in the surface waters, with luminous DOM diminishing offshore as chl-a and pH escalated. Fluorescent DOM exhibited a pronounced minimum at a sea depth of 16 meters. Turbidity exhibited a complicated geographic pattern in the estuary, with a composite estuarine visibility maximum closely associated with the halocline.

The particle size ranges of dispersed particulates exhibited two predominant modes: a minor peak at about 8 µm and a central peak ranging from around 185 µm to above the measurement capabilities of the equipment. The 9 µm mode predominated in terms of particle sizes in the top water column at open water sites C2 and D, and was detected in the near-bottom liquid at the shallow sites A and F. The 185 µm mode predominated in the particulate size ranges at shallow platforms A and F and in the halocline and sub-halocline sea layers at open-water sites C2 and D.

The spatial patterns of 9 and 185 µm particle categories in the estuary corroborate these data. Particles measuring eight micrometres were distributed diffusely in surface waters, with the highest concentration observed along the halocline interface and the sill's inner edge (5-9 m deep at station F). Particles measuring 120 and 85 micrometers were arranged in laterally constant layers a few meters thick, discernible between neighboring stations located several kilometers apart. These strata were detected at multiple depths, with the highest concentration around the halo-cline.

The particle nitrogen (PN) and phosphate (PP) levels exhibited significant variation across depth layers and size categories. PN varied between 0.12 and 4.2 umol L-1, while PP ranged from 0.02 to 0.15 umol L-1. The maximum quantities of PN and PP were detected in the subhalocline zone. The maximum values for PN were seen in the smallest category of sizes (1-4 µm), while for PP, they were found in the middle size class (4-12 µm).

The molecular proportion of nitrogen to phosphorus mirrored the fluctuation of particle nitrogen, peaking in the smallest category of sizes within the subhalocline layer. Similar to particle nutrients, levels of particle iron (Fepart) and magnesium (Mnpart) exhibited considerable variation across depth levels and size categories. Fepart levels ranged from 0.3 to 3.8 mol L-1, whereas Mpart varied from 0.06 to 7.9 umol L-1. Peak Fepart and Fepart levels were detected in the medium category of sizes (2-12 µm) inside the subhalocline level, thereby closely mirroring the scattering of PP.

Conclusion

Estuaries are centers of primary production and nutrient conversion. Despite previous studies emphasizing the significance of estuarine environments and their connections to coastal environments, the comparative impact of benthic vs aquatic activities and the effect of hypsometry on estuarine areas have seldom been measured. The extent to which an estuary provides to a neighboring coastal region via 'out-welling' of materials, along with its capacity to regulate nutrient and pollutant levels from riverine and coastal sources, is essential for ecosystem-based land-to-sea conservation. The study elucidates the response of estuarine production to evolving stressors, including heightened visibility and SLR, facilitating future management choices.

The research found that benthic sands served as a nutrient supply under illuminated and dark circumstances. The water column was a nutrient drain for almost all levels and lighting conditions. The release of minerals from the seabed enhanced the main efficiency in the water column and increased the overall discharge of living things from the estuary's surface. A net influx of minerals from the coastline into an estuary was recorded, with 12-55% greater concentrations of Dissolved Reactive Phosphorus (DRP) and Dissolved Inorganic Nitrogen (DIN) entering the estuary compared to those exiting. This, along with the overall export of Chla, indicates that soluble inorganic elements from the coast are probably assimilated by the main generators in the estuaries and transformed into particle microalgal material, a portion of which is returned to the coastline. The observations and computations, derived from a specific 24-hour sample period under ideal circumstances (summer, little rainfall), offer a distinctive representation of estuary-scale rates of nutrient shifts, change, and conveyance.

A fundamental finding of the research is that coastal and deep subtidal estuarine ecosystems significantly contribute to the total productivity of coastal ecosystems. Management must visualize the possible impacts of enduring long-term stresses such as SLR, and the estimations and basic computations endeavor to fulfill this requirement. The influence of SLR on primary manufacturing in estuaries is expected to differ according to the pace of SLR, estuary hypsometry, and degree of landward armoring, resulting in significant ambiguity on the manifestation of SLR. In the short future, facilitating the landward migration of the tide zone will mitigate the adverse effects of sea-level rise on primary output and augment the initial production in certain estuaries. Enabling landward migration thereby mitigates specific detrimental impacts of climate change. The research recommends that research on estuarine environment communities and services is essential to contextualize the findings of sea level rise forecasts, considering the significant consequences that global warming will have on managing ecosystems.

References

Agarwal, A. and Yadhav, S., 2023. Structure and Functional Guild

Composition of Fish Assemblages in the Matla Estuary, Indian Sundarbans. *Aquatic Ecosystems and Environmental Frontiers*, *1*(1), pp.16-20.

Akyol, O. and Capape, C., 2024. Capture of a new-born shortfin mako shark Isurus oxyrinchus (Lamniformes: Lamnidae), with updated records from the Turkish marine waters. *Natural and Engineering Sciences*, *9*(1), pp.1-9. https://doi.org/10.28978/nesciences.1472086

Arvinth, N., 2023. Digital Transformation and Innovation Management: A Study of How Firms Balance Exploration and Exploitation. *Global Perspectives in Management, 1*(1), pp.66-77.

Cardoso, P.G., 2022. Estuaries: dynamics, biodiversity, and impacts. In *Life Below Water* (pp. 355-366). Cham: Springer International Publishing. https://doi.org/10.1007/978-3-319-98536-7_17

Costa, Y., Martins, I., de Carvalho, G.C. and Barros, F., 2023. Trends of sea-level rise effects on estuaries and estimates of future saline intrusion. *Ocean & Coastal Management*, *236*, p.106490. https://doi.org/10.1016/j.ocecoaman.2023.106490

Dias, E., Morais, P., Antunes, C. and Hoffman, J.C., 2023. The benthic food web connects the estuarine habitat mosaic to adjacent ecosystems. *Food webs*, *35*, p.e00282. https://doi.org/10.1016/j.fooweb.2023.e00282

Farfoura, M. E., Khashan, O. A., Omar, H., Alshamaila, Y., Karim, N. A., Tseng, H. T., and Alshinwan, M., 2023. A Fragile Watermarking Method for Content-Authentication of H. 264-AVC Video. *Journal of Internet Services and Information Security*, *13*(2), pp.211-232. https://doi.org/10.58346/JISIS.2023.I2.014

Gonzalez, M. and El-Sayed, A., 2024. Impact of Terminology Standardization on Diagnostic Consistency in Multicenter Studies. *Global Journal of Medical Terminology Research and Informatics*, *2*(1), pp.13-15.

Iyengar, K. and Joshi, P., 2024. The Transformation of Gender Roles in Pastoralist Communities: An Anthropological Inquiry. *Progression journal of Human Demography and Anthropology*, *2*(3), pp.9-12.

Khojasteh, D., Glamore, W., Heimhuber, V. and Felder, S., 2021. Sea level rise impacts on estuarine dynamics: A review. *Science of The Total Environment*, *780*, p.146470. https://doi.org/10.1016/j.scitotenv.2021.146470

Mthembu, T. and Dlamini, L., 2024. Thermodynamics of Mechanical Systems Principles and Applications. *Association Journal of Interdisciplinary Technics in Engineering Mechanics*, *2*(3), pp.12-17.

Mustafa, G., Hussain, S., Liu, Y., Ali, I., Liu, J. and Bano, H., 2024. Microbiology of wetlands and the carbon cycle in coastal wetland mediated by microorganisms. *Science of The Total Environment*, p.175734. https://doi.org/10.1016/j.scitotenv.2024.175734

Myoa, Z., Pyo, H. and Mon, M., 2023. Leveraging Real-World Evidence in Pharmacovigilance Reporting.

Clinical Journal for Medicine, Health and Pharmacy, *1*(1), pp.48-63.

Nihlani, A. and Chhabda, P.K., 2024. The Impact of Digital Transformation on Supply Chain Management: A Study of How Firms Adapt. *Indian Journal of Information Sources and Services*, *14*(4), pp.1-6. https://doi.org/10.51983/ijiss-2024.14.4.01

Patankar, V. and Kapoor, M., 2024. Process Optimization of Filtration in Crystallization-Based Product Recovery. *Engineering Perspectives in Filtration and Separation*, *2*(1), pp.5-8.

Rahman, M.A., Pramanik, M.M.H., Hasan, M.M., Ahmed, T., Alam, M.A., Hasan, S.J., Rahman, B.M.S., Haidar, M.I., Rashid, M.H., Zaher, M. and Khan, M.H., 2024. Sixth sanctuary identification research and establishment strategy for enhancing production and conservation management of Hilsa (Tenualosa ilisha) in Bangladesh. *International Journal of Aquatic Research and Environmental Studies*, pp.37-47. https://doi.org/10.70102/IJARES/V4I1/4

Ranjan, A., and Bhagat, S., 2024. Multilateral Partnerships for Clean Water Access an Evaluation of SDG 6 Collaborations. *International Journal of SDG's Prospects and Breakthroughs*, *2*(3), pp.1-3.

Robles, T., Alcarria, R., De Andrés, D.M., De la Cruz, M.N., Calero, R., Iglesias, S., and Lopez, M., 2015. An IoT based reference architecture for smart water management processes. *Journal of Wireless Mobile Networks, Ubiquitous Computing, and Dependable Applications*, *6*(1), pp.4-23.

Rullens, V., Mangan, S., Stephenson, F., Clark, D.E., Bulmer, R.H., Berthelsen, A., Crawshaw, J., Gladstone-Gallagher, R.V., Thomas, S., Ellis, J.I. and Pilditch, C.A., 2022. Understanding the consequences of sea level rise: the ecological implications of losing intertidal habitat. *New Zealand Journal of Marine and Freshwater Research*, *56*(3), pp.353-370. https://doi.org/10.1080/00288330.2022.2086587

Shakya, A.W. and Allgeier, J.E., 2023. Water column contributions to coral reef productivity: overcoming challenges of context dependence. *Biological Reviews*, *98*(5), pp.1812-1828. https://doi.org/10.1111/brv.12984

Smihunova, O., Bohdaniuk, I., Polyakova, Y., and Yehiozarian, A., 2024. Innovative Approaches to Controlling in Agribusiness: The Role of Quality Management Systems in Sustainable Production Practices. *Archives for Technical Sciences*, *2*(31), pp.116–130. https://doi.org/10.70102/afts.2024.1631.116

Soares, C.C., Galiforni-Silva, F. and Winter, C., 2024. Representative residual transport pathways in a mixed-energy open tidal system. *Journal of Sea Research*, *201*, p.102530. https://doi.org/10.1016/j.seares.2024.102530